

## Cell toxic damages during polycyclic aromatic hydrocarbons biodegradation by *Pseudomonas aeruginosa* G24

Huan Gao <sup>a,b</sup>, Manli Wu <sup>a,b,c,\*</sup>, Heng Liu <sup>a,b</sup>, Ting Zhang <sup>a,b</sup>, Xuhong Zhang <sup>a,b</sup>

<sup>a</sup> Shaanxi Key Laboratory of Environmental Engineering, Xi'an University of Architecture and Technology, Xi'an 710055, People's Republic of China

<sup>b</sup> Key Laboratory of Northwest Water Resource, Environment and Ecology, MOE, Xi'an University of Architecture and Technology, Xi'an 710055, People's Republic of China

<sup>c</sup> School of Environmental and Civil Engineering, Xi'an University of Architecture and Technology, Xi'an 710055, People's Republic of China

### ARTICLE INFO

**Keywords:**

*Pseudomonas aeruginosa* G24  
Polycyclic aromatic hydrocarbons (PAHs)  
Cellular characteristics  
Biodegradation  
Toxic damages

### ABSTRACT

Many microorganisms are capable of degrading polycyclic aromatic hydrocarbons (PAHs), but the extent of toxicity of PAHs on these degraders is not yet fully understood. In this study, the physicochemical responses of the PAH-degrading strain *Pseudomonas aeruginosa* (*P. aeruginosa*) G24 under PAHs stress were investigated. After 21 days of incubation, the total removal rates of phenanthrene (Phe) and pyrene (Pyr) by *P. aeruginosa* G24 were 43.8 % and 36.8 %, respectively. Among them, about 11 % of PAHs were absorbed by pellets in the molecular form, resulting in net biodegradation rates of 32.9 % and 25.2 % for Phe and Pyr, respectively. Further investigations revealed that the surface zeta potential of the *P. aeruginosa* G24 increased from 16.78 to 19.31 mV to 30.32–33.59 mV, the percentage of permeable cells increased from 24.5 %-32.5 % to 52.4 %-56.2 %, and the EPS contents decreased from 2.34 to 3.37 mg L<sup>-1</sup> to 0.63–1.80 mg L<sup>-1</sup> in the “Phe-MSM + *P. aeruginosa* G24” and “Pyr-MSM + *P. aeruginosa* G24” systems. The damages of *P. aeruginosa* G24 during PAH degradation included increased zeta potential and permeability on the bacterial surface, increased cell apoptosis, reduced EPS contents, as well as injured cell membrane structures. The findings of the study suggest that the damages or apoptosis of *P. aeruginosa* G24 may inhibit the continuous degradation of residual PAHs during the late stage of incubation.

## 1. Introduction

Polycyclic aromatic hydrocarbons (PAHs) are persistent toxic and recalcitrant pollutants in the environment [1–3]. Due to their affordability and environmental friendliness, isolating strains that are capable of degrading PAHs is a common method of PAH remediation [4–6]. Previous studies on PAH biodegradation mostly focused on the isolation of degrading strain, optimization of degradation conditions, enhancement of removal efficiencies, as well as analysis of degradation pathway [1,4,5,7–9].

*Pseudomonas* is the most common PAH-degrading species isolated from hydrocarbon-polluted environments such as oilfields and coking plants [10–12]. Numerous studies have reported that the *Pseudomonas aeruginosa* (*P. aeruginosa*) has a remarkable ability to degrade a huge spectrum of persistent organic pollutants (POPs), including PAHs, phenolic compounds, alkanes, and nitrogenous organic compounds.

*P. aeruginosa* can improve hydrocarbon biodegradation processes through various pathways including oxidation, dehydrogenation, hydroxylation and reduction, and produce biosurfactants to enhance bioavailability [13–15]. Sunita and Vivek [16] reported that *P. aeruginosa* NCIM 5514 has unique properties of carbon spectrum utilization and can degrade 76.14 % of oily waste in 56 days. Moreover, Zhang et al. [17] found that *P. aeruginosa* DQ8 was capable of degrading both n-alkanes and PAHs with three or four aromatic rings.

Microbial activity is one of the key factors influencing PAHs biodegradation efficiency [18–20]. In general, microbes develop elaborate responses to release external signals and adjust their metabolic capacities to cope with pollutant stress [21]. The cell membrane is the initial interface and the major site for metabolic reactions of various substances, which can affect the biosorption and transmission of pollutants ([22] ; [19]). Bacterial activity and reproductive growth are also crucial factors to ensure efficient decomposition of contaminants

\* Corresponding author at: Shaanxi Key Laboratory of Environmental Engineering, Xi'an University of Architecture and Technology, Xi'an 710055, People's Republic of China.

E-mail address: [wumanli1974@hotmail.com](mailto:wumanli1974@hotmail.com) (M. Wu).

[23].

Flow cytometry is a fast and convenient method that can distinguish damaged cells from living cells, providing valuable insights into cellular states at different times. Apoptosis is a cellular regulatory mechanism that allows microorganisms to adjust their body functions, resist adverse environments, and re-adapt to new living conditions through a series of metabolic adjustments [24]. By measuring changes in apoptosis, the cellular response mechanism under pollution stress can be revealed. Changes in the charge on the surface of bacterial cells can be used to understand the interaction between pollutants and bacteria, and the influence of pollution on cell surface structures can be further understood by measuring the Zeta potential value of bacteria [25]. Furthermore, changes in cell morphology and internal structure can result in the loss of cell function when microorganisms are exposed to toxic substances [26]. Therefore, it is important to study the changes in cellular microstructure during microbial degradation to reveal the physiological and biochemical reactions of cells during pollutant remediation. The characteristic Fourier transform infrared (FTIR) spectral measurements can provide insight into the condition of injured microbes and the types of injuries that occur. Environmental stresses, such as exposure to organic pollutants, can damage the bacterial cell membrane, proteins, and nucleic acid components, triggering physiological reactions in bacterial cells. These reactions may lead to the production of specific protein compounds that exhibit unique absorption in the FTIR region and provide distinctive characteristics of bacterial damage [27].

The exploration of the toxic effects of PAHs on microbial cells during degradation was complemented by attempts to investigate their protection mechanisms in the PAHs environment. It is known that extracellular polymeric substances (EPS) play a dominant role in organism protection. However, the potential protective mechanisms of EPS for PAHs degradation by *P. aeruginosa* have been poorly studied, and the positive role in protecting microorganisms from environmental stresses has not been elucidated.

In this study, a PAH-degrading strain, *P. aeruginosa* G24, was isolated from petroleum-contaminated soil collected from the northern of Shaanxi province of China. The response of *P. aeruginosa* G24 to PAHs (phenanthrene, pyrene) with different benzene ring structures was revealed, with special emphasis on the role of EPS. The main objectives of this study were to (1) investigate PAH biodegradation effects by *P. aeruginosa* G24; (2) characterize changes in the biochemical properties of *P. aeruginosa* G24, including functional group structures, zeta potential, surface structure, and extracellular polymer under PAHs environment; (3) explore the relationship between cell damage and PAH degradation; and (4) elucidate the protective mechanisms of EPS in response to the PAHs environment. This study contributed to a better understanding of the damage effects of *P. aeruginosa* during PAHs biodegradation.

## 2. Materials and methods

### 2.1. Isolation of PAH-degrading strain *Pseudomonas aeruginosa* G24

Five gram of petroleum-contaminated soil, collected from the northern region of Shaanxi province in China, was added to 50 mL of sterile mineral salt medium (MSM). The MSM consisted of 0.27 g K<sub>2</sub>HPO<sub>4</sub>, 0.35 g KH<sub>2</sub>PO<sub>4</sub>, 2.7 g NH<sub>4</sub>Cl, 0.1 g MgCl<sub>2</sub>·6H<sub>2</sub>O, 0.1 g CaCl<sub>2</sub>·2H<sub>2</sub>O, 0.009 g FeCl<sub>2</sub>·4H<sub>2</sub>O, 0.004 g MnCl<sub>2</sub>·4H<sub>2</sub>O in 1 L sterile water with pH adjusted to 7.0. 5 mL of 1.0 g L<sup>-1</sup> phenanthrene (Phe) and pyrene (Pyr) (obtained from Sigma-Aldrich, St. Louis, MO, USA, with dichloromethane as solvent) were added to the cultures as the sole carbon source. The experiment was conducted at room temperature (25–30 °C) with a shaking incubator set to 150 rpm. After 7 days of incubation, 5 mL of the culture was transferred to another sterile 50 mL MSM medium containing 100 mg L<sup>-1</sup> Phe and Pyr and incubated for 7 days under the same conditions. The enriched culture was subcultured for 5 cycles of enrichment to obtain the consortia cultures capable of

degrading PAHs.

The PAHs-degrading consortia cultures were then serially diluted, and the strain screening was performed on sterile MSM agar plates with 100 mg L<sup>-1</sup> Phe and Pyr as the sole carbon source. Phenotypically distinct colonies were collected and purified using the streak plate method. All plates were incubated at 30 °C for 2 to 3 days. Afterwards, colonies with different morphologies were streaked on the PAHs-MSM agar plates, and this step was repeated three times. After selecting a single colony of the isolate, that exhibited continuous growth on the plates, as the potential PAHs degrader, it was suspended in PBS buffer consisting of 8.0 g NaCl, 1.42 g Na<sub>2</sub>HPO<sub>4</sub>, 0.27 g KH<sub>2</sub>PO<sub>4</sub>, 0.2 g KCl, and 1 L sterile water. The PAHs degrading bacteria were identified through 16S ribosomal RNA (16S rRNA) gene sequencing and compared with the Ez-Taxon database of EZBioCloud® (ChunLab, Korea). The sequence obtained in this study was deposited in the GenBank database with the accession number OP268283.

### 2.2. Experimental designs

The detailed experimental design schematic is shown in Supplementary S1. In brief, the experiments were conducted in eighteen 50 mL Erlenmeyer flasks divided into six groups with three parallel samples for each group. First, 20 mL of MSM were added to each flask and autoclaved at 121 °C, then 10<sup>8</sup> CFU mL<sup>-1</sup> of *P. aeruginosa* G24 was respectively added to systems (1)–(4), while 10 mg L<sup>-1</sup> Phe, Pyr, and glucose (Glu) were respectively added to systems (2), (3), and (4). System (5) contained 20 mL of MSM plus 10 mg L<sup>-1</sup> Phe, and system (6) contained 20 mL of MSM plus 10 mg L<sup>-1</sup> Pyr. Thus, six systems were set up to evaluate the PAHs biodegradation and the bacterial cytotoxic response of *P. aeruginosa* G24 including (1) MSM + *P. aeruginosa* G24 (blank), (2) Phe-MSM + *P. aeruginosa* G24, (3) Pyr-MSM + *P. aeruginosa* G24, (4) Glu-MSM + *P. aeruginosa* G24, (5) Phe + MSM, and (6) Pyr + MSM. The experiment ran for 21 days, and all treatments were incubated at room temperature (25 °C) in a rotating shaking incubator at 120 rpm. All experiments were conducted in triplicate.

### 2.3. PAHs determination

#### 2.3.1. The total removal rates of Phe and Pyr in the systems

After 2, 4, 7, and 21 days of incubation, Phe in the systems of “(2) Phe-MSM + *P. aeruginosa* G24” and “(5) Phe + MSM”, and Pyr in the systems of “(3) Pyr-MSM + *P. aeruginosa* G24” and “(6) Pyr + MSM” were extracted repeatedly three times using cyclohexane. The resulting extracts were dried over anhydrous sodium sulfate, concentrated, and filtered prior to Gas Chromatography Mass Spectrometer (GC-MS) analysis [28]. The Phe and Pyr concentrations were determined using an Agilent 7010 GC-MS system (USA) equipped with a HP-5 column (30 m × 0.32 mm × 0.25 µm). Helium was used as the carrier gas with a flow rate of 1.50 mL min<sup>-1</sup>. The column temperature program started at 40 °C and was held for 2 min, after which the oven was heated to 110 °C at a rate of 35 °C min<sup>-1</sup>, followed by an increase to 129 °C at 15 °C min<sup>-1</sup> and continued to be heated to 270 °C with a rate of 20 °C min<sup>-1</sup>. Finally, the temperature reached 280 °C and was held for 5 min. The total removal rates of Phe and Pyr were calculated using Eq. (1).

$$\text{PAHs removal (\%)} = \frac{C_0 - C_n}{C_0} \times 100\% \quad (1)$$

where C<sub>0</sub> is the initial concentration of Phe or Pyr (mg L<sup>-1</sup>), and C<sub>n</sub> is the residual concentration of Phe or Pyr in the system (mg L<sup>-1</sup>).

#### 2.3.2. The biodegradation rates of phenanthrene and pyrene in the systems

To determine the intracellular concentrations of Phe and Pyr in *P. aeruginosa* G24, thalli were collected from the systems “(2) Phe-MSM + *P. aeruginosa* G24” or “(3) Pyr-MSM + *P. aeruginosa* G24” after 2, 4, 7, and 21 days of incubations by centrifugation at 8000 rpm

for 15 min. The thalli were then suspended in 20 mL of sterile MSM medium and disrupted using an ultrasonic sonifier (TL-650Y, China). Intracellular Phe or Pyr was extracted using cyclohexane and the process was repeated three times. The intracellular Phe or Pyr contents ( $C_{\text{intracellular}}$ ) were determined using GC-MS (Agilent 7010, USA) as described in Section 2.3.1. The biodegradation rates of Phe and Pyr were calculated using Eq. (2):

$$\text{Biodegradation}(\%) = \frac{C_0 - C_n - C_{\text{intracellular}}}{C_0} \times 100\% \quad (2)$$

where  $C_0$  is the initial concentration of PAHs ( $\text{mg L}^{-1}$ ),  $C_n$  is the residual concentration of PAHs in the systems ( $\text{mg L}^{-1}$ ), and  $C_{\text{intracellular}}$  is the residual concentration of PAHs in intracellular ( $\text{mg L}^{-1}$ ).

### 2.3.3. Quality control and quality assurance

The quantitative analysis of Phe and Pyr was carried out using the external standard method. The mother liquor of Phe and Pyr was diluted step by step with cyclohexane, a series of concentrations of 100, 500, 1000, 2000, 5000, 10,000  $\mu\text{g L}^{-1}$  were prepared for determination, and the standard curve was plotted with the concentration as the horizontal coordinate and the peak area as the vertical coordinate. The detection limit of the method was set as the content of Phe and Pyr corresponding to the 3-fold signal-to-noise ratio (S/N). To determine the recoveries of each substance, the blank MSM was spiked with a Phe and Pyr solution at a concentration of 1000  $\mu\text{g L}^{-1}$ , and was treated three times in parallel.

As shown in Supplementary Table S1, the correlation coefficients  $R^2$  ranged from 0.9883 to 0.9979 in the concentration range of 100–10,000  $\mu\text{g L}^{-1}$ , demonstrating that Phe and Pyr exhibited good linearity within this concentration range. In addition, the detection limits of both substances were lower than 0.6  $\mu\text{g L}^{-1}$ , and the recoveries were 97.3 % (Phe) and 102.3 % (Pyr), indicating that the method has good reproducibility and accuracy.

### 2.4. FTIR, SEM and zeta potential analysis

**Fourier Transform infrared spectroscopy (FTIR)** analysis was conducted to obtain the structural variation information of *P. aeruginosa* G24 following the method of Yin et al. [29]. After 4 and 15 days of incubation, *P. aeruginosa* G24 were respectively collected from systems (1), (2), (3), and (4) by centrifugation at 6000 rpm for 10 min at 4 °C. After washing three times with PBS buffer, the thalli were freeze-dried for 24 h and subjected to infrared spectroscopy (FTIR Thermo, IS50, USA) with a detection wavenumber range of 4000–600  $\text{cm}^{-1}$ .

**Scanning Electron Microscope (SEM)** analysis was performed to examine *P. aeruginosa* G24 in the systems of (1), (2), (3), and (4). First, thalli were separately collected, washed twice with ultrapure water, and fixed with 2.5 % glutaraldehyde overnight. They were then dehydrated in ethanol/acetone (1/1), and then fixed with 1 % starvation acid before being treated with gold spray. Finally, images were taken and recorded using a scanning electron microscope (SEM, JSM-6510LV, Japan) [30].

**Zeta potential analysis** was performed on *P. aeruginosa* G24 samples from systems (1), (2), (3), and (4). The samples were collected through centrifugation at 6000 rpm for 10 min, washed with a 10  $\text{mmol L}^{-1}$  phosphate buffer solution, and then suspended in 50 mL of PBS buffer and shaken to ensure uniformity [31]. The zeta potential was measured using a zeta potential meter (Nano-Zetasizer Malvern, UK).

### 2.5. EPS extraction and 3D-EEM spectra analysis

The extracellular polymers (EPS) were extracted from *P. aeruginosa* G24 pellets collected from systems (1), (2), (3), and (4) by centrifugation three times at 5000 rpm for 10 min using a modified hot alkali method according to Zou [32]. The granules were washed with 0.9 % NaCl solutions, and pH values were adjusted to 7.0 with 0.1 mol  $\text{L}^{-1}$  NaOH. The

extracts were then heated to 80 °C in a water bath for 30 min, and then centrifuged at 5000 rpm for 20 min. The resulting supernatants were filtered with 0.45  $\mu\text{m}$  Millipore membranes for further three-dimension excitation emission matrix fluorescence spectroscopy (3D-EEM spectra) analysis [33].

The 3D-EEM spectra were measured using the F-7000 fluorescence spectrophotometer (Hitachi Co., Japan), equipped with a 150 W xenon arc lamp as the excitation (Ex) source. Spectra were recorded at a scan rate of 2400 nm  $\text{min}^{-1}$  using Ex and emission (Em) slit bandwidths of 5 nm, and the wavelengths were set from 200 to 550 nm for both Ex and Em. A photomultiplier tube voltage of 400 V was applied for low-level light detection. Sigma Plot software (Systat Software Inc., USA) was used to obtain the 3D-EEM spectra.

### 2.6. Flow cytometric measurements

The bacterial cells were harvested from systems (1), (2), (3), and (4) and washed twice with high purity water. The cells were then suspended in 200  $\mu\text{L}$  binding buffer with 5  $\mu\text{L}$  Annexin V-FITC and incubated in the dark at room temperature for 10 min. The cell pellets were collected by centrifugation at 1000 rpm for 5 min, suspended in binding buffer, and stained with PI for 15 min at room temperature in the dark. Flow cytometry was used to assay apoptosis, with the control being bacteria that were treated in the same way as the experimental group but not stained. All flow cytometric measurements (FCM) data were processed using the BD Accuri CFlow software.

The effects of pollutants on bacterial cells were detected using a flow cytometer (Accuri C6, BD, USA) equipped with double solid-state laser emitting at wavelengths of 488 nm and 640 nm. Annexin V-FITC fluorescence and PI fluorescence were collected in FL1 and FL2 channels, respectively. Measurements were performed at an affixed flow rate of 10  $\mu\text{L min}^{-1}$ . The detection range of the flow cytometer applied in the study was  $10^3$ – $10^5$  CFU  $\text{mL}^{-1}$ , and therefore the sample suspensions were diluted with ultrapure water as necessary.

### 2.7. Statistical analysis

Student's *t*-tests were performed to determine if there were any significant differences (*p*-value <0.05) in the concentrations of PAHs between the samples.

## 3. Results

### 3.1. Total removal rates and biodegradation rates of PAHs

The total removal rates of PAHs in the systems were calculated using Eq. (1), while the biodegradation rates of PAHs (excluding the cellular swallowing part) were calculated using Eq. (2), and the results are presented in Fig. 1.

During the 7 days of incubation in the systems of "Phe-MSM + *P. aeruginosa* G24" and "Pyr-MSM + *P. aeruginosa* G24", the total removal rates of Phe and Pyr were 38.8 % and 29.4 %, respectively. The PAH degradation rates slowed down after 7 days, and the total removal rates increased to 43.8 % (Phe) and 36.8 % (Pyr) after 21 days of degradation. In the blank systems (Phe-MSM or Pyr-MSM systems), only 4.91 % of Phe and 3.28 % of Pyr were removed (Not shown in Fig. 1). These results suggest that *P. aeruginosa* G24 was capable of degrading PAHs in the MSM medium.

After 21 days of incubations, the amounts of Phe and Pyr swallowed by *P. aeruginosa* G24 pellets were found to be 0.0218 mg and 0.0232 mg in the "Phe-MSM + *P. aeruginosa* G24" and "Pyr-MSM + *P. aeruginosa* G24" systems, respectively. This indicated that Phe and Pyr were not completely mineralized into carbon dioxide and water by *P. aeruginosa* G24, and that parts of PAHs were transferred from the solution into the pellets through "intracellular swallowing". Thus, the biodegradation rates of Phe and Pyr were 32.9 % and 25.2 %, respectively, which were

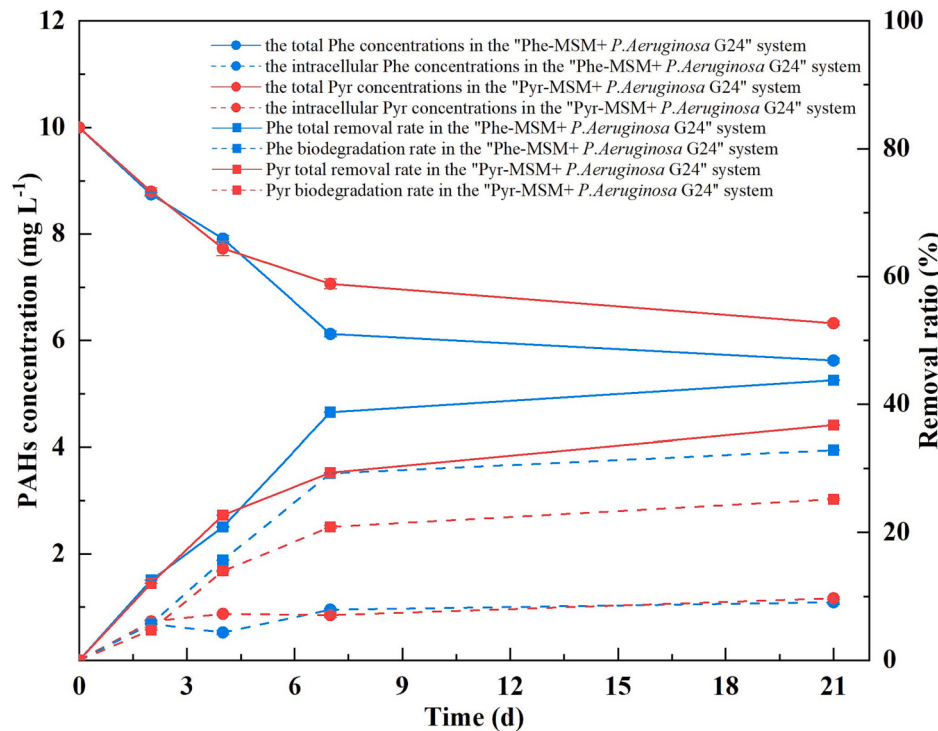


**Fig. 1.** Phenanthrene (Phe) and pyrene (Pyr) biodegradation and total removal rates by *P. aeruginosa* G24. Blue circle-solid line means the total Phe concentrations in the liquid phase (mg L⁻¹); blue circle-dotted line means the Phe contents in the intracellular of *P. aeruginosa* G24 (mg L⁻¹). Red circle-solid line means the total Pyr concentrations in the liquid phase (mg L⁻¹); red circle-dotted line means the Pyr contents in the intracellular of *P. aeruginosa* G24 (mg L⁻¹). Blue square-solid line means the Phe removal ratio (%); blue square-dotted line means the Phe biodegradation ratio (%). Red square-solid line means the Pyr removal ratio (%); Red square-dotted line means the Pyr biodegradation ratio (%). (For interpretation of the references to colour in this figure legend, the reader is referred to the web version of this article.)

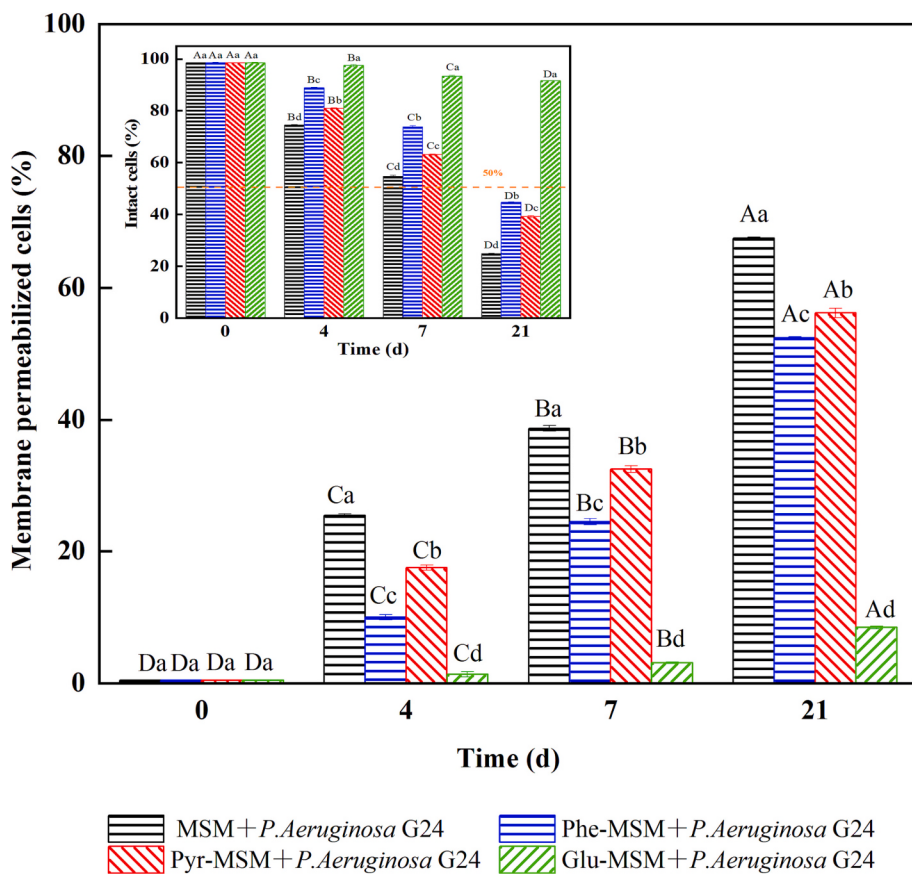


**Fig. 2.** Membrane permeabilized of *P. aeruginosa* G24 cells in the systems of “MSM + *P. aeruginosa* G24”, “Phe-MSM + *P. aeruginosa* G24”, “Pyr-MSM + *P. aeruginosa* G24”, “Glu-MSM + *P. aeruginosa* G24” on days of 0, 4, 7 and 21 d separately. The insert shows intact *P. aeruginosa* G24 cells. Capital letters stands for the significant differences of zeta potential in different times in the same system; lower letters stands for the significant differences of zeta potential in different systems at the same time.

lower than their total removal rates.

### 3.2. Biochemical properties of *P. aeruginosa* G24 under PAH stress

#### 3.2.1. Cell membrane permeability

The variation in membrane permeability detected by FCM in the “Phe–MSM + *P. aeruginosa* G24”, “Pyr–MSM + *P. aeruginosa* G24”, “Glu–MSM + *P. aeruginosa* G24” and “MSM + *P. aeruginosa* G24” systems was investigated, and the results are presented in Fig. 2.

In the “Phe–MSM + *P. aeruginosa* G24” and “Pyr–MSM + *P. aeruginosa* G24” systems, the percentage of membrane permeabilized cells was found to be 10.02 % and 17.5 %, respectively, during the first four days of incubations. This percentage increased to 24.5 % and 32.5 % on the 7th day, and finally to 52.4 % and 56.2 % on the 21st day. While the proportions of membrane permeabilized cells in the “MSM + *P. aeruginosa* G24” system also increased from 25.5 % to 67.5 %, it was only 8.45 % in the “Glu–MSM + *P. aeruginosa* G24” system after 21 days of incubation.

This result was also visually demonstrated by characterization through the FTIR and SEM analyses of *P. aeruginosa* G24 in different cultural media (Figs. S2, S3). After 21 days of incubation, the cells appeared shrunk and rough in the “MSM + *P. aeruginosa* G24” and “Glu–MSM + *P. aeruginosa* G24” systems, while cells became ruptured and even developed “cavity” in the “Phe–MSM + *P. aeruginosa* G24” and “Pyr–MSM + *P. aeruginosa* G24” systems. SEM results demonstrated that the damage of *P. aeruginosa* G24 cells was more severe under PAH stress than with glucose acting as the carbon source (Fig. S2). Further analysis revealed that the functional groups on the surface of the four systems changed in the later stage. The absorption peaks in the spectral region ( $1200\text{--}900\text{ cm}^{-1}$ ) representing the molecular structure of peptidoglycan, lipopolysaccharide, and phosphoric acid decreased significantly

on the surface of the strains of “Phe–MSM + *P. aeruginosa* G24”, “Pyr–MSM + *P. aeruginosa* G24”, and “MSM + *P. aeruginosa* G24” systems. The peak patterns representing DNA/RNA, fatty acids, and Amide II also decreased. However, the decrease of bacteria surface absorption peak was relatively small in the “glucose + *P. aeruginosa* G24” system (Fig. S3). These results suggest that the changes in the toxic carbon sources caused by the changes of phosphoric acid molecular skeleton, fatty acid, and protein in cell membrane structure led to the destruction of the cell membrane structure, indicating that the permeability of the cell membrane was destroyed under PAHs. This could lead to the PAHs biodegradation stagnation at the late stage of incubation.

#### 3.2.2. Surface zeta potential of the *P. aeruginosa* G24

The surface zeta potential of *P. aeruginosa* G24 was determined in the four systems, including “MSM + *P. aeruginosa* G24”, “Phe–MSM + *P. aeruginosa* G24”, “Pyr–MSM + *P. aeruginosa* G24”, and “Glu–MSM + *P. aeruginosa* G24” on days of 0, 4, 7, and 21, as shown in Fig. 3. In the “MSM + *P. aeruginosa* G24” system, the surface zeta potential values of *P. aeruginosa* G24 increased slightly from 16.78 mV (day 0) to 19.32 mV (day 21). In the “Glu–MSM + *P. aeruginosa* G24” system, the surface zeta potential values fluctuated and remained in the range of 16.01–17.83 mV. Notably, in the “Phe–MSM + *P. aeruginosa* G24” and “Pyr–MSM + *P. aeruginosa* G24” systems, the surface zeta potential values of the bacteria increased significantly to 30.32 mV and 33.59 mV, respectively, after 21 days of incubation.

#### 3.2.3. Cell apoptosis of *P. aeruginosa* G24

The apoptosis rates were found to be 36.6 % ( $p < 0.05$ ) in the “Phe–MSM + *P. aeruginosa* G24” and 43.3 % ( $p < 0.05$ ) in the “Pyr–MSM + *P. aeruginosa* G24” systems, while they were 53.1 % ( $p < 0.05$ ) and 11.3 % ( $p < 0.05$ ) in the “MSM + *P. aeruginosa* G24” and “Glu–MSM +

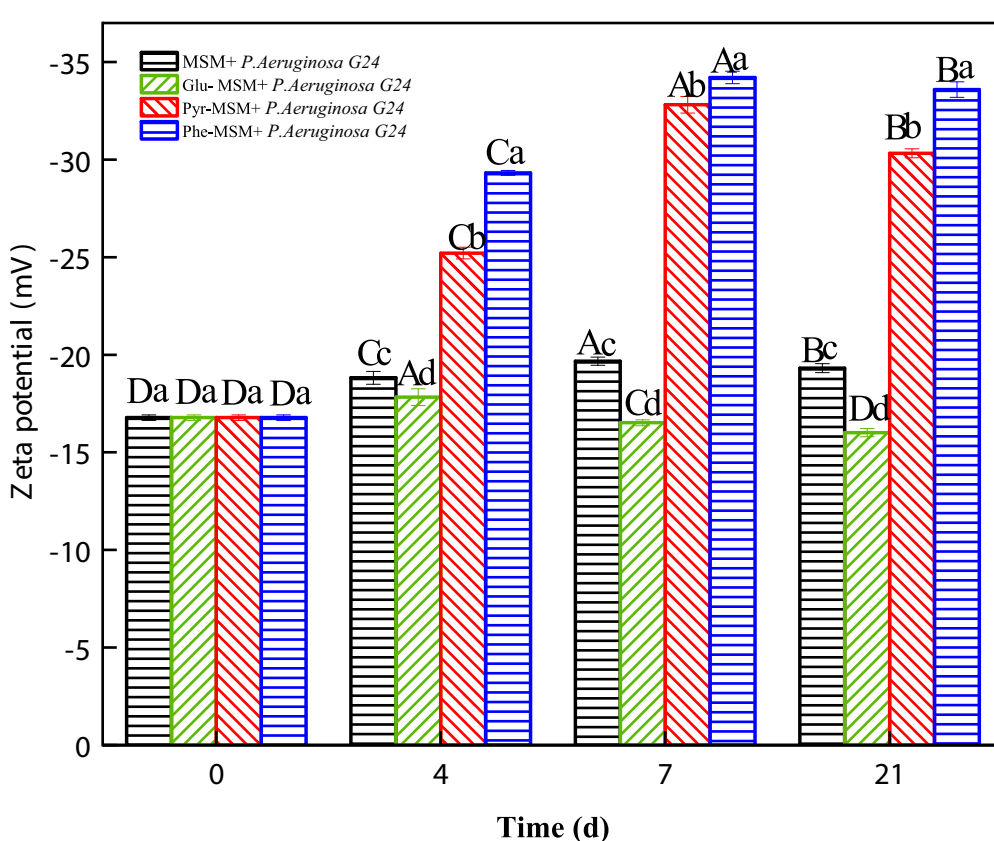


**Fig. 3.** The zeta potential of the four systems including “MSM + *P. aeruginosa* G24”, “Phe–MSM + *P. aeruginosa* G24”, “Pyr–MSM + *P. aeruginosa* G24”, “Glu–MSM + *P. aeruginosa* G24” on days of 0, 4, 7 and 21 d, separately. The capital letters stands for the significant differences of zeta potential during different times in the same system; the lower letters means the significant differences of zeta potential in different systems at the same time.

*P. aeruginosa* G24” systems, respectively, during 4 days of incubations. After 21 days of incubation, the cell apoptosis rates increased significantly and reached 73.9 % ( $p < 0.05$ ), 79.9 % ( $p < 0.05$ ), and 82.4 % ( $p < 0.05$ ) in the “Phe–MSM + *P. aeruginosa* G24”, “Pyr–MSM + *P. aeruginosa* G24”, and “MSM + *P. aeruginosa* G24” systems, respectively, whereas only 16.1 % ( $p < 0.05$ ) apoptosis was observed in the “Glu–MSM + *P. aeruginosa* G24” system (Fig. 4). This result indicates that the absence of a carbon source led to the highest cell apoptosis rates, followed by the systems with toxic PAHs as carbon sources. Conversely, the lowest apoptosis rate was observed in the system with glucose as the sole carbon source. This implies that while microorganisms can proliferate by metabolizing Phe and Pyr, the toxicity of PAHs also caused damage to cells.

### 3.3. Protective mechanisms

As shown in Fig. 5a, the EPS contents decreased with the incubation time in the same system. After 4 days of incubation, the EPS contents were 2.34 and 3.37 mg L<sup>-1</sup> in the “Phe–MSM + *P. aeruginosa* G24” and “Pyr–MSM + *P. aeruginosa* G24” systems, respectively, and then decreased to 0.63 and 1.80 mg L<sup>-1</sup> after 21 days of incubations.

The fluorescence spectra of EPS in Fig. 5b showed that at the initial incubation stages, protein-like and tryptophan-like substances were present in the EPS, indicated by the appearance of peaks at 350–425 nm/425–475 nm in both systems after 4 and 7 days of incubation. After 21 days, the peaks at the same wavelengths indicated the presence of humic acid substances produced in both systems at the later stage of incubation. The contents of protein-like, tryptophan-like, and humic acids of EPS in the two systems varied during the incubation process. The protein-like and tryptophan-like substances peaks in the “Phe–MSM + *P. aeruginosa* G24” system were the strongest after 7 days of incubations, while the humic acid substance peak in the “Pyr + *P. aeruginosa* G24” systems was the strongest after 21 days.

## 4. Discussion

It has been found that PAHs degradation rates slowed down and a stagnation period occurred in the later stage of biodegradation which may lead to the residue of PAHs remaining in the environment. Mishra et al. [34] reported *Actinobacterium* genera degraded up to 81 % of Phe within 72 h of incubation, but degradation rates decreased in the late stage, resulting in a final degradation efficiency of 87 % at 168 h. Similarly, Lu et al. [35] observed an initial removal rate of 43.8 % within 48 h of PAH degradation by *M. extorquens* C1, followed by stagnation at 72 h.

Some literatures suggested that PAH biodegradation stagnation may be due to the insufficient supply of carbon source substrates or the toxicity of intermediate metabolites [35,41]. Wang et al. [41] found that the highest PAH degradation occurred in a system where glucose acted as the co-metabolism carbon sources, inducing the strain to produce more biofilm to adapt to the hydrophobic environment. Lu et al. [35] speculated that the sorption of coumarin, resveratrol, and rutin into the bacteria may be attributed to their polar groups combined to the lipopolysaccharide or fatty acid structures in the cell wall or cell membranes, which causes an increase in cell surface hydrophobicity, increasing the sorption of PAHs onto the surface of cells.

In the systems of “Phe–MSM + *P. aeruginosa* G24” and “Pyr–MSM + *P. aeruginosa* G24”, the possible fates of Phe and Pyr include: (1) being biodegraded and mineralized into carbon dioxide and water by *P. aeruginosa* G24; (2) being “swallowed into” the pellets of *P. aeruginosa* G24 and still existing in molecular form; (3) remaining in the MSM medium in molecular form. In this study, “the total removal rates” were greater than the “biodegradation rates” of PAHs, and about 20 % of PAHs were swallowed by the strain and entered the cells (Fig. 1). These intracellular Phe and Pyr may produce toxic effects on the bacteria, impeding further PAH biodegradation.

Cell membrane permeability is associated with cell damage. The greater the permeability of the cell membrane, the more serious the cell

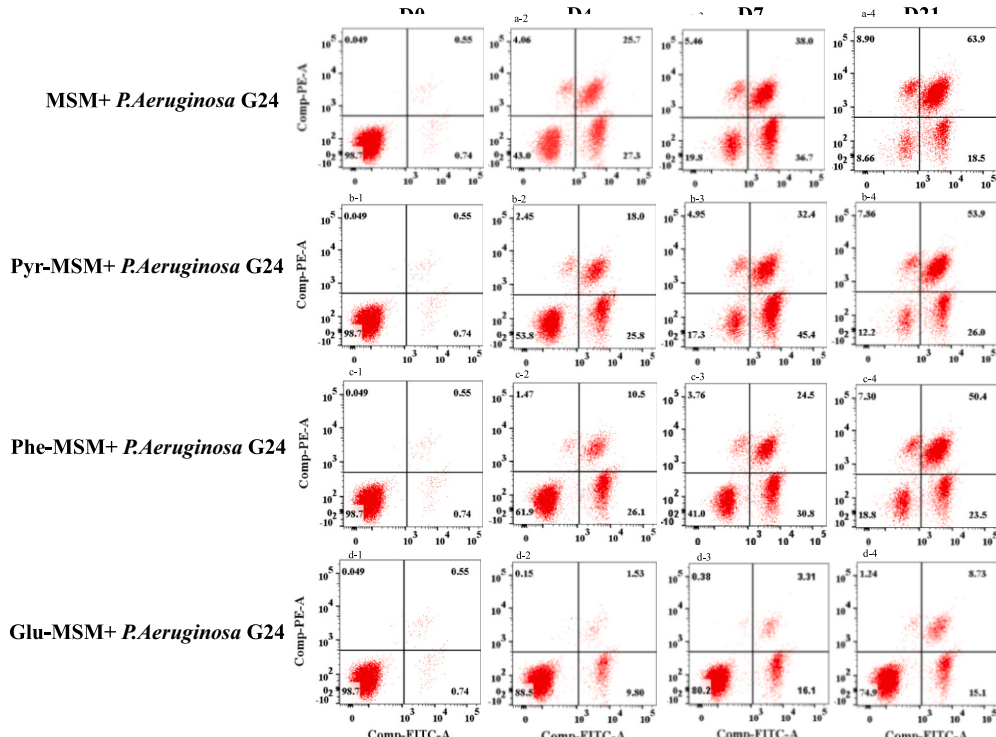


**Fig. 4.** The apoptosis of *P. aeruginosa* G24 in the “MSM + *P. aeruginosa* G24” “Pyr–MSM + *P. aeruginosa* G24”, “Phe–MSM + *P. aeruginosa* G24”, “Glu–MSM + *P. aeruginosa* G24” systems on 0, 4, 7 and 21 days, separately. Upper left/UL means cell debris; Upper right/UR means the late stage of apoptotic cells; Lower Right/LR means the early stage of apoptosis cells.

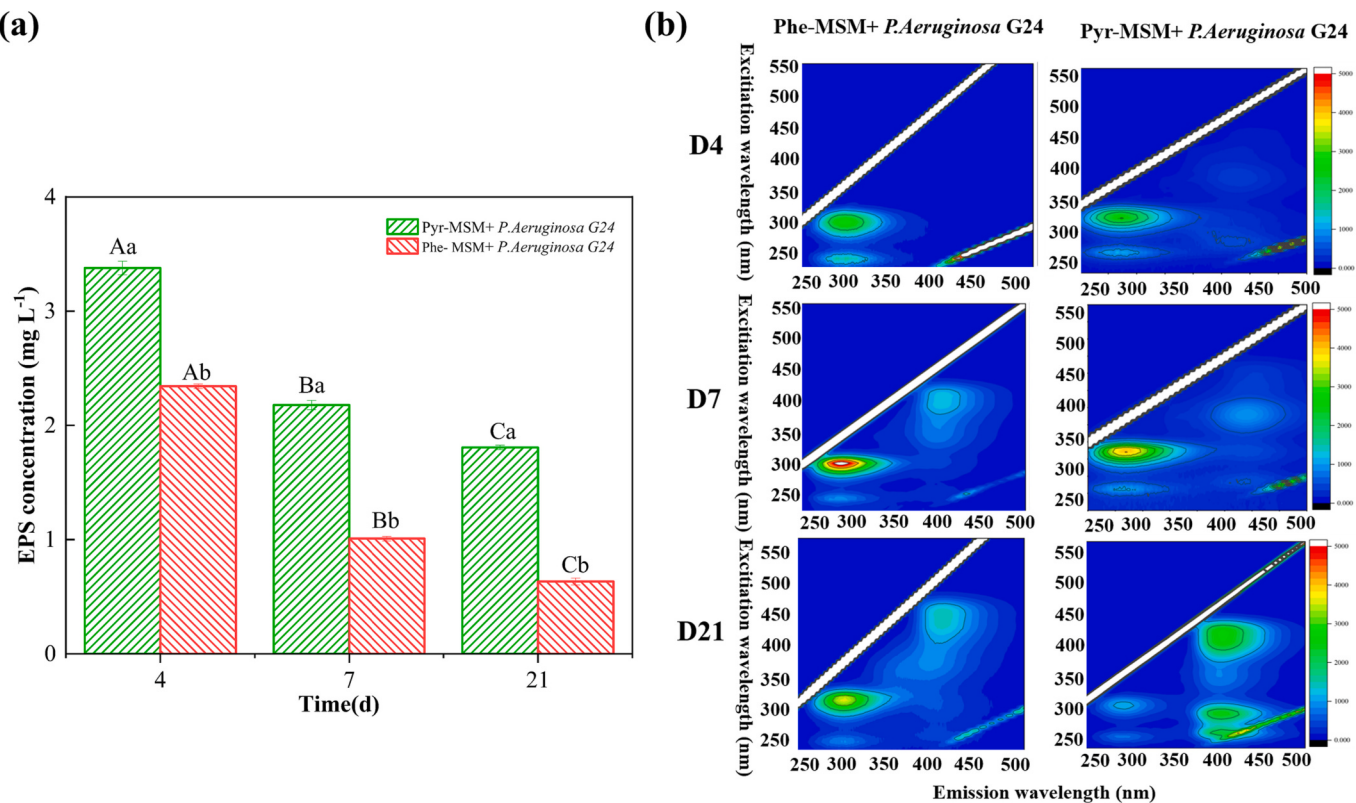


**Fig. 5.** (a) The EPS contents in the systems of “Phe-MSM + *P. aeruginosa* G24” and “Pyr-MSM + *P. aeruginosa* G24” on 4, 7 and 21 days, separately. The capital letters stands for the significant differences during different periods in the same systems; the lower letters stands for the significant differences in different systems at the same time; (b) Fluorescence excitation–emission matrix spectra of EPS in the systems of “Phe-MSM + *P. aeruginosa* G24” and “Pyr-MSM + *P. aeruginosa* G24” on 4, 7 and 21 days, separately. The peaks at Ex/Em 225–325/275–325 nm stands for tryptophan & protein-like substance; the peaks at Ex/Em 275–425/375–450 nm associated with soluble microbial by-products, fulvic acid-like; the peaks at Ex/Em 350–500/400–450 nm stands for humic acid-like substance.

damage or rupture [42]. The cell membrane was found to be more permeable in the system with PAHs as the carbon source than in the glucose system. This indicates that PAHs as a carbon source disrupted the permeability of *P. aeruginosa* G24 cells, ultimately leading to PAH slow degradation stagnation at the late stage of incubation (Fig. 2).

The SEM and FTIR analyses (Figs. S2, S3) further demonstrated that during the 15-day incubation period in the Phe-MSM- *P. aeruginosa* G24” and “Pyr-MSM- *P. aeruginosa* G24” systems, the bacterial cell surface became rough, the cytoplasm density decreased, and even the cell ruptured and developed “cavity”. This indicates that the PAHs altered the permeability of the cell membrane which may lead to the degradation stagnation of PAHs [36].

The impact of toxic substances on bacterial activity could be determined by measuring changes in the surface potential of the strain. Previous studies have suggested that the zeta potential of the bacterial surface increased when using the disinfectant to sterilize pathogenic bacteria in water [37]. Additionally, Cristin et al. [38] and Wang et al. [39] reported that the accumulation of pollutants led to cell rupture, apoptosis, and a decrease in the negative charge on the bacterial surface. In this study, the zeta potential of the *P. aeruginosa* G24 was higher in the “Phe –MSM+ *P. aeruginosa* G24” and “Pyr –MSM+ *P. aeruginosa* G24” systems as compared to the system using glucose as a carbon source or the blank without carbon source. Glucose, a high-quality carbon source, did not cause obvious changes in the cell surface charge. These results indicate that the damage or apoptosis of *P. aeruginosa* G24 during PAHs degradation led to an increase in zeta potential on the bacterial surface, which may affect the continuous degradation of residual PAHs (Fig. 3).

Apoptosis is the most common mechanism of cell death that microorganisms use to adjust their cell functions and resist adverse environments through a series of metabolic responses [24]. In the systems of

“Phe-MSM+ *P. aeruginosa* G24” and “Pyr-MSM+ *P. aeruginosa* G24”, *P. aeruginosa* G24 cells initiated their own stress regulation in order to adapt to the adverse environments. This resulted in changes to the cell membrane system, increased plasma membrane permeability, and eventually, autonomic apoptosis (Fig. 4). With the decomposition of cells, necessary nutrients were provided for other cells with stronger vitality in the system, promoting the adsorption of pollutants. Therefore, the degradation rate of Phe and Pyr by *P. aeruginosa* G24 increased rapidly in the early stage of degradation. However, at the later stage of degradation, most of the cells had already undergone advanced stages of apoptosis, indicating that most of the cells in the system had been inactivated by toxic accumulation.

In the presence of *P. aeruginosa* G24, it is likely that microbes respond acutely to PAHs by binding them through the EPS (Fig. 6). With increasing degradation time, the active sites may become depleted, and the protective action of the EPS may gradually diminish, potentially leading to membrane rupture due to the accumulation of contaminant toxicity. Notably, it was also observed that the degradation efficiency of Phe was higher than that of Pyr, suggesting that while four-ring PAHs may induce microbes to produce more EPS in the extracellular space to reduce pollutant stress, their higher toxicity accelerated cell apoptosis. This finding is consistent with previous studies.

At the early stage of PAH degradation, the EEM results indicated that tryptophan-like substance were the main components of EPS. This may indicate an adaptive mechanism in which the secretion of tryptophan-like substance is enhanced, potentially serving as a means for microbes to ease the chemical stress of PAHs. Due to this possible protective pathway, *P. aeruginosa* G24 can still be capable of degradation when exposed to high ring PAH system.

However, the levels of tryptophan-like substances decreased while

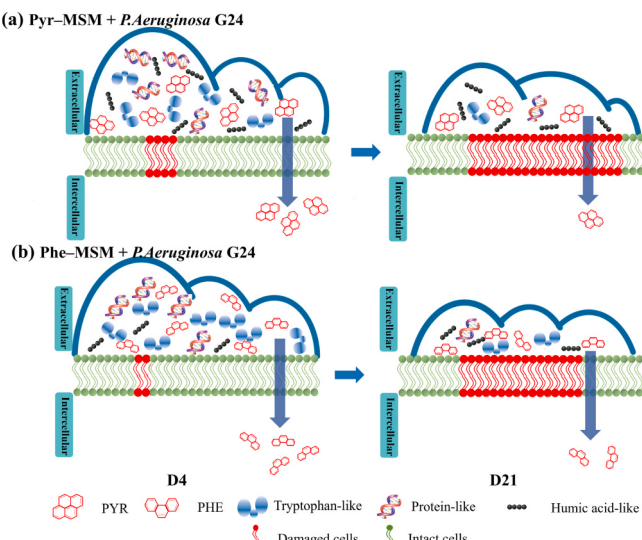


**Fig. 6.** Schematic diagram of protective mechanisms potentially occurred in the systems of “Phe-MSM + *P. aeruginosa* G24” and “Pyr-MSM + *P. aeruginosa* G24”.

humus-like substances were generated at the late stage of incubation (Fig. 6). It has been reported that humic acids are associated with the growth of certain bacteria, macromolecular organics, and the disintegration of dead cells [40]. Thus, these results suggested that the EPS abatement and humus-like substances generation may have contributed to the occurrence of PAH degradation stagnation.

## 5. Conclusions

In this study, the cellular toxic effects of *P. aeruginosa* G24 during PAHs biodegradation could effectively be alleviated through production of tryptophan-like substances at the early stage of incubation. However, the accumulation of PAHs in the intracellular of *P. aeruginosa* G24 led to the cell damages including enhancement the zeta potential and permeability on the bacterial surface, and reduction of EPS contents, as well as the cell apoptosis. These cellular toxic effects impeded the continuous degradation of residual PAHs during the late stage of incubation. More detailed studies on the protective mechanisms of microbial extracellular enzymes in the PAHs environment need to be conducted in the future.

## CRediT authorship contribution statement

Huan Gao: Methodology, Formal analysis, Writing-Original draft preparation. Manli Wu: Conceptualization, Writing-Reviewing and Editing. Heng Liu: Visualization, Investigation. Ting Zhang: Visualization, Investigation. Xuhong Zhang: Visualization.

## Declaration of competing interest

The authors declare that they have no known competing financial interests or personal relationships that could have appeared to influence the work reported in this paper.

## Data availability

No data was used for the research described in the article.

## Acknowledgments

The authors gratefully acknowledge the support of the National Natural Science Foundation of China (No. 52070154 and No.

21577109).

## Appendix A. Supplementary data

Supplementary data to this article can be found online at <https://doi.org/10.1016/j.jwpe.2023.103992>.

## References

- [1] C.L. Davie-Martin, K.G. Stratton, J.G. Teeguarden, K.M. Waters, S.L.M. Simonich, Implications of bioremediation of polycyclic aromatic hydrocarbon-contaminated soils for human health and cancer risk, Environ. Sci. Technol. 51 (2017) 9458–9468, <https://doi.org/10.1021/acs.est.7b02956>.
- [2] I.A. Titaley, S.L.M. Simonich, M. Larsson, Recent advances in the study of the remediation of polycyclic aromatic compound (PAC)-contaminated soils: transformation products, toxicity, and bioavailability analyses, Environ Sci Tech Let. 7 (2020) 873–882, <https://doi.org/10.1021/acs.estlett.0c00677>.
- [3] L.S.D. Trine, E.L. Davis, C. Roper, L. Truong, R.L. Tanguay, S.L.M. Simonich, Formation of PAH derivatives and increased developmental toxicity during steam enhanced extraction remediation of creosote contaminated superfund soil, Environ. Sci. Technol. 53 (2020) 4460–4469, <https://doi.org/10.1021/acs.est.8b07231>.
- [4] E.R. Rene, C. Kennes, L.D. Nghiem, S. Varjani, New insights in biodegradation of organic pollutants, Bioresour. Technol. 347 (2022), 126737, <https://doi.org/10.1016/j.biortech.2022.126737>.
- [5] A.K. Rathankumar, K. Saikia, P.S. Kumar, S. Varjani, S. Kalita, N. Bharadwaj, J. George, V. Kumar, Surfactant aided mycoremediation of soil contaminated with polycyclic aromatic hydrocarbon (PAHs): progress, limitation and countermeasures, J Chem Technol Biot. 97 (2022) 391–408, <https://doi.org/10.1002/jctb.6721>.
- [6] Sakshi, S.K. Singh, A.K. Haritash, Catabolic enzyme activities during biodegradation of three-ring PAHs by novel DTU-1Y and DTU-7P strains isolated from petroleum-contaminated soil, Arch. Microbiol. 203 (2021) 3101–3110, <https://doi.org/10.1007/s00203-021-02297-4>.
- [7] C. Chen, W. Lei, M. Lu, J. Zhang, Z. Zhang, C. Luo, Y. Chen, Q. Hong, Z. Shen, Characterization of Cu(II) and Cd(II) resistance mechanisms in *Sphingobium* sp. PHE-SPH and *Ochrobactrum* sp. PHE-OCH and their potential application in the bioremediation of heavy metal-phenanthrene co-contaminated sites, Environ. Sci. Pollut. Res. 23 (2016) 6861–6872, <https://doi.org/10.1007/s11356-015-5926-0>.
- [8] A.B. Patel, T. Manvar, K.R. Jain, C. Desai, D. Madamwar, Metagenomic insights into bacterial communities' structures in polycyclic aromatic hydrocarbons degrading consortia, J Environ Chem Eng. 9 (2021), 106578, <https://doi.org/10.1016/j.jece.2021.106578>.
- [9] Sakshi, S.K. Singh, A.K. Haritash, Catabolic enzyme activity and kinetics of pyrene degradation by novel bacterial strains isolated from contaminated soil, Environmental Technology & Innovation. 23 (2021), 101744, <https://doi.org/10.1016/j.eti.2021.101744>.
- [10] H. Liu, R. Liang, F. Tao, C. Ma, Y. Liu, X. Liu, J. Liu, Genome sequence of *Pseudomonas aeruginosa* strain SJTD-1, a bacterium capable of degrading long-chain alkanes and crude oil, J. Bacteriol. 194 (2012) 4783–4784, <https://doi.org/10.1128/JB.01061-12>.
- [11] Z. Fathi, G. Ebriahimipour, Isolation and identification of polycyclic aromatic hydrocarbons (PAHs) degrading bacteria from Arak Petrochemical Wastewater, J Microb. Biotechnol. Food. 7 (5) (2018) 499–504, <https://doi.org/10.15414/jmbf.2018.7.5.499-504>.
- [12] P.A. Patel, V.V. Kothari, C.R. Kothari, P.R. Faldu, K.K. Domadia, C.M. Rawal, H. D. Bhimanji, N.R. Parmar, N.M. Nathani, P.G. Koringa, C.G. Joshi, R.K. Kothari, Draft genome sequence of petroleum hydrocarbon-degrading *Pseudomonas aeruginosa* strain PK6, isolated from the Saurashtra region of Gujarat, India, Genome Ann. 2 (2014) 2–14, <https://doi.org/10.1128/genomeA.00002-14>.
- [13] F.A. Bezza, E.M.N. Chirwa, The role of lipopeptide biosurfactant on microbial remediation of aged polycyclic aromatic hydrocarbons (PAHs)-contaminated soil, Chem. Eng. J. 309 (2017) 563–576, <https://doi.org/10.1016/j.cej.2016.10.055>.
- [14] L. Ohno-Machado, NIH's big data to knowledge initiative and the advancement of biomedical informatics, J Am Med Inform Assn. 21 (2014) 193, <https://doi.org/10.1136/amiajnl-2014-002666>.
- [15] S. Pourfadakari, M. Ahmadib, N. Jaafarzadeh, A. Takdastan, A.A. Neisi, S. Ghafari, S. Jorfi, Remediation of PAHs contaminated soil using a sequence of soil washing with biosurfactant produced by *Pseudomonas aeruginosa* strain PF2 and electrokinetic oxidation of desorbed solution, effect of electrode modification with Fe<sub>3</sub>O<sub>4</sub> nanoparticles, J. Hazard. Mater. 379 (2019), 120839, <https://doi.org/10.1016/j.jhazmat.2019.120839>.
- [16] J.V. Sunita, N.U. Vivek, Carbon spectrum utilization by an indigenous strain of *Pseudomonas aeruginosa* NCIM 5514: production, characterization and surface active properties of biosurfactant, Bioresour. Technol. 221 (2016) 510–516, <https://doi.org/10.1016/j.biortech.2016.09.080>.
- [17] Z.Z. Zhang, Z.W. Hou, C.Y. Yang, C.Q. Ma, F. Tao, P. Xu, Degradation of n-alkanes and polycyclic aromatic hydrocarbons in petroleum by a newly isolated *Pseudomonas aeruginosa* DQ8, Bioresour. Technol. 102 (5) (2011) 4111–4116, <https://doi.org/10.1016/j.biortech.2010.12.064>.
- [18] K. Dercova, K. Laszlova, H. Dudasova, S. Murinova, M. Balascakova, J. Skarba, The hierarchy in selection of bioremediation techniques: the potentials of utilizing

- bacterial degraders, *Chem. List.* 109 (4) (2015) 281–290, <https://doi.org/10.1016/j.colsurfb.2017.06>.
- [19] N. Golani-Rozen, B. Seiwert, C. Riemenschneider, T. Reemtsma, B. Chefetz, Y. Hadar, Transformation pathways of the recalcitrant pharmaceutical compound carbamazepine by the white-rot fungus *Pleurotus ostreatus*: effects of growth conditions, *Environ. Sci. Technol.* 49 (20) (2015) 12351–12362, <https://doi.org/10.1021/acs.est.5b02222>.
- [20] Sakshi, S.K. Singh, A.K. Haritash, Bacterial degradation of mixed-PAHs and expression of PAH-catabolic genes, *World J Microb Biot.* 39 (2022) 47, <https://doi.org/10.1007/s11274-022-03489-w>.
- [21] N.S. Kudryasheva, A.S. Tarasova, Pollutant toxicity and detoxification by humic substances: mechanisms and quantitative assessment via luminescent biomonitoring, *Environ. Sci. Pollut. Res.* 22 (1) (2015) 155–167, <https://doi.org/10.1007/s11356-014-3459-6>.
- [22] Z. Molatová, E. Skrivanová, B. Macias, N.R. Mcewan, P. Brézina, M. Marounek, Susceptibility of *Campylobacter jejuni* to organic acids and monoacylglycerols, *Folia Microbiol.* 55 (3) (2010) 215–220, <https://doi.org/10.1007/s12223-010-0031-8>.
- [23] F. David, A. Berger, R. Hansch, M. Rohde, E. Franco-Lara, Single cell analysis applied to antibody fragment production with *Bacillus megaterium*: development of advanced physiology and bioprocess state estimation tools, *MicrobCell Fact.* 10 (2011) 23, <https://doi.org/10.1186/1475-2859-10-23>.
- [24] X.B. Jin, H.F. Mei, X.B. Li, Y. Ma, A.H. Zeng, Y. Wang, X.M. Lu, F.J. Chu, Q. Wu, J. Y. Zhu, Apoptosis-inducing activity of the antimicrobial peptide cecropin of *Musca domestica* in human hepatocellular carcinoma cell line BEL-7402 and the possible mechanism, *Acta BiochBioph Sin.* 42 (4) (2010) 259–265, <https://doi.org/10.1093/abbs/gmq021>.
- [25] A.J. Wynessa, D.M. Paterson, E.C. Defew, M.I. Stutter, L.M. Avery, The role of zeta potential in the adhesion of *E. coli* to suspended intertidal sediments, *Water Res.* 142 (2018) 159–166, <https://doi.org/10.1016/j.watres.2018.05.054>.
- [26] J.S. Ye, H. Yin, D.P. Xie, H. Peng, J. Huang, W.Y. Liang, Copper biosorption and ions release by *Stenotrophomonas maltophilia* in the presence of benzo[a]pyrene, *Chem. Eng. J.* 219 (2013) 1–9, <https://doi.org/10.1016/j.cej.2012.12.093>.
- [27] K. Madhuree, K. Siya, C. Jayabaskaran, Uinic acid induced changes in biomolecules and their association with apoptosis in squamous carcinoma (A-431) cells: a flow cytometry, FTIR and DLS spectroscopic study, *S A P: M&S B.* 274 (2022), 121098, <https://doi.org/10.1016/j.saa.2022.121098>.
- [28] B.G. Haren, Z.P. Hares, G.P. Payal, C.P. Ajay, S. Alka, V. Sunita, P.D. Bharti, Exploring bacterial communities through metagenomics during bioremediation of polycyclic aromatic hydrocarbons from contaminated sediments, *Sci. Total Environ.* 842 (2022), 156794, <https://doi.org/10.1016/j.scitotenv.2022.156794>.
- [29] C. Yin, F. Meng, G.H. Chen, Spectroscopic characterization of extracellular polymeric substances from a mixed culture dominated by ammonia-oxidizing bacteria, *Water Res.* 68 (2015) 740–749, <https://doi.org/10.1016/j.watres.2014.10.046>.
- [30] M.K. Li, Z.G. He, Y.T. Hu, L. Hu, H. Zhong, Both cell envelope and cytoplasm were the locations for chromium (VI) reduction by *Bacillus* sp. M6, *Bioresour. Technol.* 273 (2019) 130–135, <https://doi.org/10.1016/j.biortech.2018.11.006>.
- [31] J. Qi, Y.Y. Ye, J.J. Wu, H.T. Wang, F.T. Li, Dispersion and stability of titanium dioxide nanoparticles in aqueous suspension: effects of ultrasonication and concentration, *Water Sci. Technol.* 67 (2013) 147–151, <https://doi.org/10.2166/wst.2012.545>.
- [32] X. Zou, Study on extraction of extracellular polymeric substances from same sludge under different conditions, *J. Environ. Sci.* 4 (2) (2010) 436–440, <https://doi.org/10.1016/j.ese.2012.100212>.
- [33] Q. He, Z. Yuan, J. Zhang, S. Zhang, W. Zhang, Z. Zou, H. Wang, Insight into the impact of ZnO nanoparticles on aerobic granular sludge under shock loading, *Chemosphere* 173 (2017) 411–416, <https://doi.org/10.1016/j.chemosphere.2017.01.085>.
- [34] A. Mishra, R. Rathour, R. Singh, T. Kumari, I.S. Thakur, Degradation and detoxification of phenanthrene by actinobacterium *Zhihengliuella* sp. ISTPL4, *Environ Sci Pollut R.* 27 (2020) 27256–27267, <https://doi.org/10.1007/s11356-019-05478-3>.
- [35] L. Lu, Q.C. Chai, S.Y. He, C.P. Yang, D. Zhang, Effects and mechanisms of phytoalexins on the removal of polycyclic aromatic hydrocarbons (PAHs) by an endophytic bacterium isolated from ryegrass, *Environ. Pollut.* 253 (2019) 872–881, <https://doi.org/10.1016/j.envpol.2019.07.097>.
- [36] Y. Zhong, T.G. Luan, L. Lin, H. Liu, N.F.Y. Tam, Production of metabolites in the biodegradation of phenanthrene, fluoranthene and pyrene by the mixed culture of *Mycobacterium* sp. and *Sphingomonas* sp., *Bioresour. Technol.* 102 (2011) 2965–2972, <https://doi.org/10.1016/j.biortech.2010.09.113>.
- [37] S.J. Ye, Z.H. He, G.F. Hong, Z.S. Tian, X.Y. Shi, Influence of chemical disinfectants on zeta potential of free bacteria surface in sewage treatment systems, *Chinese J Disinfection.* 23 (2006) 415–418, <https://doi.org/10.3969/j.issn.1001-7658.2006.05.011>.
- [38] P. Cristin, F. Turci, M. Tomatis, M. Ghiazza, D. Lison, B. Fubini, Z potential evidences silanol heterogeneity induced by metal contaminants at the quartz surface: implications in membrane damage, *Colloid Surface B.* 157 (449) (2017) 455, <https://doi.org/10.1016/j.colsurfb.2017.06.012>.
- [39] W.L. Wang, J.L. Zhang, Z.Q. Qiu, Z.Y. Cui, N.Q. Li, X. Li, Y.W. Wang, H.X. Zhang, C. Y. Zhao, Effects of polyethylene microplastics on cell membranes: a combined study of experiments and molecular dynamics simulations, *J. Hazard. Mater.* 429 (2022), 128323, <https://doi.org/10.1016/j.jhazmat.2022.128323>.
- [40] F. Qu, H. Liang, J. He, J. Ma, Z. Wang, H. Yu, G. Li, Characterization of dissolved extracellular organic matter (dEOM) and bound extracellular organic matter (bEOM) of *Microcystis aeruginosa* and their impacts on UF membrane fouling, *Water Res.* 46 (9) (2012) 2881–2890, <https://doi.org/10.1016/j.watres.2012.02.045>.
- [41] J.F. Wang, H. Zhang, J. Cai, J. Li, B.H. Sun, F.Y. Wu, Effects of different carbon substrates on PAHs fractions and microbial community changes in PAHs-contaminated soils, *Environ. Pollut.* 324 (2023) 121367, <https://doi.org/10.1016/j.envpol.2023.121367>.
- [42] M.M.T. Khan, B.H. Pyle, A.K. Camper, Specific and rapid enumeration of viable but nonculturable and viable-cultural gram-negative bacteria by using flow cytometry, *Appl. Environ. Microbiol.* 76 (2010) 5088–5096, <https://doi.org/10.1128/aem.02932-09>.